



## **Comparison of steady-state and transient thermo-mechanical responses of unprotected aluminum columns at elevated temperatures**

Jean C. Batista Abreu<sup>1</sup>, Nicholas A. Soares<sup>2</sup>, Tyler D. Spinello<sup>3</sup>, Ronald D. Ziemian<sup>4</sup>

### **Abstract**

In modern construction, aluminum is often used as a structural material due to its relatively high strength-to-weight ratio, resistance to corrosion, and architecturally pleasing finish. For instance, aluminum has been an important component for the development of skyscrapers atriums and exterior facades, as aluminum structures can weigh up to sixty percent less than similar steel structures with comparable strength. However, the thermo-mechanical behavior of aluminum makes design against building fires challenging, mainly because aluminum has a low melting point, and experimental data and analysis-based models for fire design are limited. Generally, steady-state and transient tests are used to determine material properties at high temperatures. In a steady-state test, a tensile specimen is heated up to a target temperature, and then subjected to axial load under constant temperature. Alternatively, a transient tensile test is completed by applying static axial load to the specimen, and then gradually heating the material to realistically simulate fire conditions. Results from steady-state tests are easier to obtain and, therefore, more commonly used in computational models. This project investigates the accuracy of numerical results obtained through “transient” models that adopt steady-state mechanical properties to study the effects of fire on aluminum structures. Thin-walled columns were analyzed using nonlinear finite element models with mechanical properties from steady-state and transient tests. Results from Abaqus collapse analyses are used to compare the load-carrying capacities and critical temperatures of slender and non-slender hollow members. Parametric studies were completed to characterize the impact of member slenderness and geometric imperfections on the stability of hollow aluminum columns at elevated temperatures.

### **1. Introduction**

Since the advent of the modern domes in the early 20<sup>th</sup> century, architects and engineers have investigated new materials that are light weight but also strong enough to support these long-span structures. Aluminum has always been a prime candidate for this purpose, however, one of its major drawbacks is its relatively low melting point and, therefore, low fire resistance.

---

<sup>1</sup> Assistant Professor, Elizabethtown College, <batistajc@etown.edu>

<sup>2</sup> Research Assistant, Bucknell University, <nas017@bucknell.edu>

<sup>3</sup> Research Assistant, Elizabethtown College, <spinellot@etown.edu>

<sup>4</sup> Professor, Bucknell University, <ziemian@bucknell.edu>

Limited research has focused on the thermo-mechanical response of aluminum members at elevated temperatures, up to its melting point of  $\sim 660$  °C (Skejić et al., 2015). Several studies focus on quantifying the degradation of the elastic modulus, 0.2 % offset stress and ultimate strength at elevated temperatures through steady-state tensile tests. During steady-state tests, the specimen is heated up to a target temperature, and then subjected to axial load until failure. In contrast, during transient tests, axial load is initially applied to the specimen, and then it is heated up with the given temperature rate, until failure. Typically, steady-state tensile tests are more commonly performed because they are easier to complete; however, they are not as realistic as transient-state tests in terms of replicating fire conditions, as structures would already be subjected to dead and live loads when a fire arises.

In practice, design manuals and codes for metal structures offer temperature-dependent mechanical properties obtained through steady-state tests, which, in some cases, can over predict the load-carrying capacity of members at elevated temperatures. The aim of this research is to numerically investigate and compare the steady-state and transient responses of 6060-T66 aluminum alloy sections at elevated temperatures using finite element models. The models, which were developed using a computational software package (Abaqus, 2018), were validated against an experimental study by Maljaars et al. (2009a), in which compression tests were conducted on slender aluminum members.

## 2. Methodology

This section describes the parameters utilized and methodology followed to complete and validate the investigation of aluminum hollow members at elevated temperatures.

### 2.1 Mechanical Properties

Mechanical properties for the 6060-T66 aluminum alloy were obtained from several sources, for comparison. The first were stress-strain curves from steady-state tensile tests and transient compression tests documented in the validation study (Maljaars et al., 2009a). Digitizing software (Mitchell et al., 2018) was used to extract the data from each stress-strain curve (Fig. 1), and then Eq. 1-2 were applied to obtain true stresses and strains.

$$\sigma_{true} = \sigma(1 + \epsilon) \quad (1)$$

$$\epsilon_{true} = \ln(1 + \epsilon) \quad (2)$$

In these equations,  $\sigma$  is axial stress, and  $\epsilon$  is the axial strain.

Linear regression was applied to fit a trendline to the initial linear portion of each curve to determine the elastic modulus,  $E$ . Roughly 30 data points were used to fit each trendline to minimize error from the data extraction, while ensuring that the coefficient of variation R-squared value was close to unity, with the lowest being 0.9924. Properties from the Aluminum Design Manual (2015) were also used for comparison. The retention factors for yield (0.2 % offset) stress are shown in Fig. 2.

Thermal expansion effects were included in all models, using an expansion coefficient of  $23.4 \times 10^{-6}$  1/°C. Thermal expansion was modeled to obtain a more accurate displacement behavior;

however, thermal expansion did not have a significant effect on the ultimate load or critical temperature given that the members were free to axially expand.

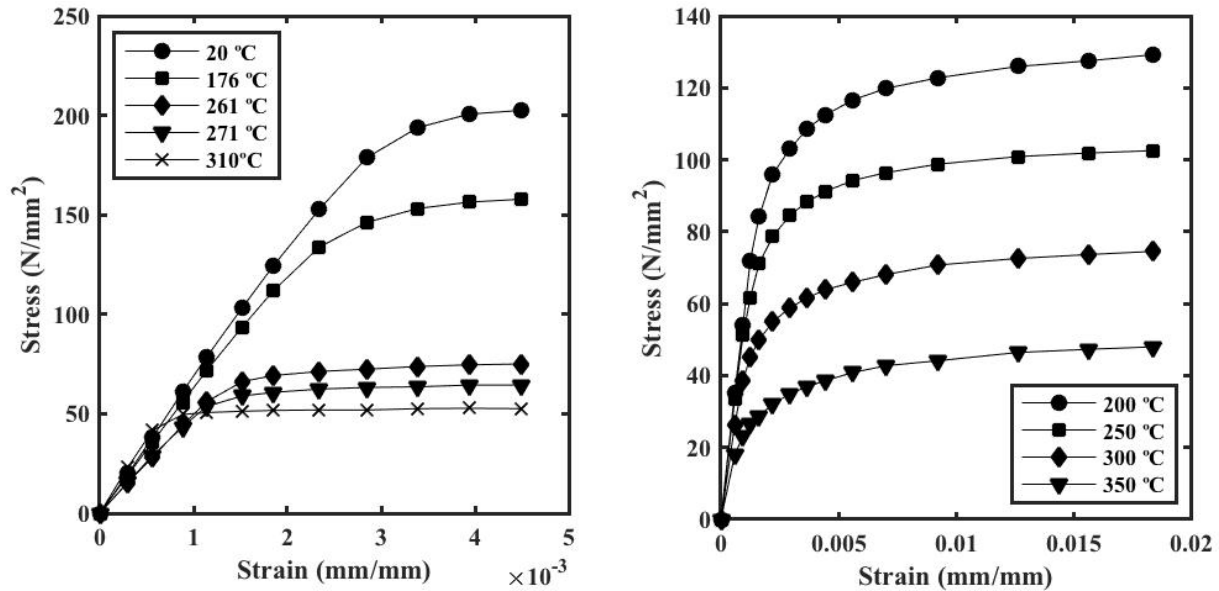


Figure 1: Stress-strain curves for aluminum alloy 6060-T66 from steady-state tensile (left) and transient compression (right) tests

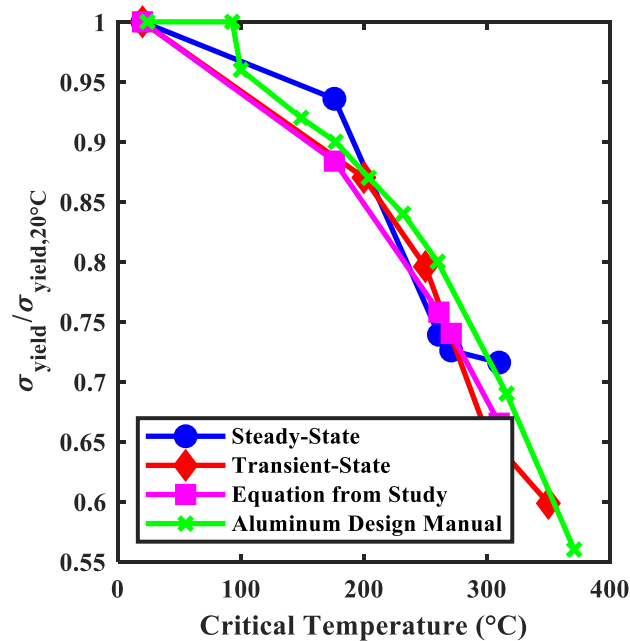


Figure 2: Retention factors for the yield (0.2 % offset) stress of aluminum 6060-T66 from steady-state and transient tension tests (Maljaars et al., 2009a), equations from this study, and Aluminum Design Manual (2015)

## 2.2 Geometry and Imperfections

The model used for validation was a hollow square tube with a width of 48.03 mm, a thickness of 1.106 mm, and a length of 300 mm. In Abaqus, the element type used was S8R (i.e. quadratic shell with reduced integration). A mesh convergence study was conducted prior to testing, and it was determined that a common element size of 2 mm could be used for all models. This provided

less than 1% difference in the ultimate load and critical temperature when compared to using nearly five times as many nodes (Fig. 3). A total of 43,392 nodes and 14,400 elements were used to validate the model shown in Fig. 4 against experimental (Maljaars et al., 2009a) and numerical (Maljaars et al., 2009b) results.

Elastic buckling analysis was performed to use the first elastic buckling mode as the shape or seed of the geometric imperfections (Fig. 5), as suggested by the reference study (Maljaars et al., 2009b). The “buckle” step was used in Abaqus, with three eigenmodes requested. After verifying the first buckling mode was local, the imperfections were scaled by the amplitude provided in the reference study. An average imperfection amplitude-to-thickness ratio of 4.28 % was determined using the data provided in the reference study, and used to estimate the imperfection as a function of the thickness.

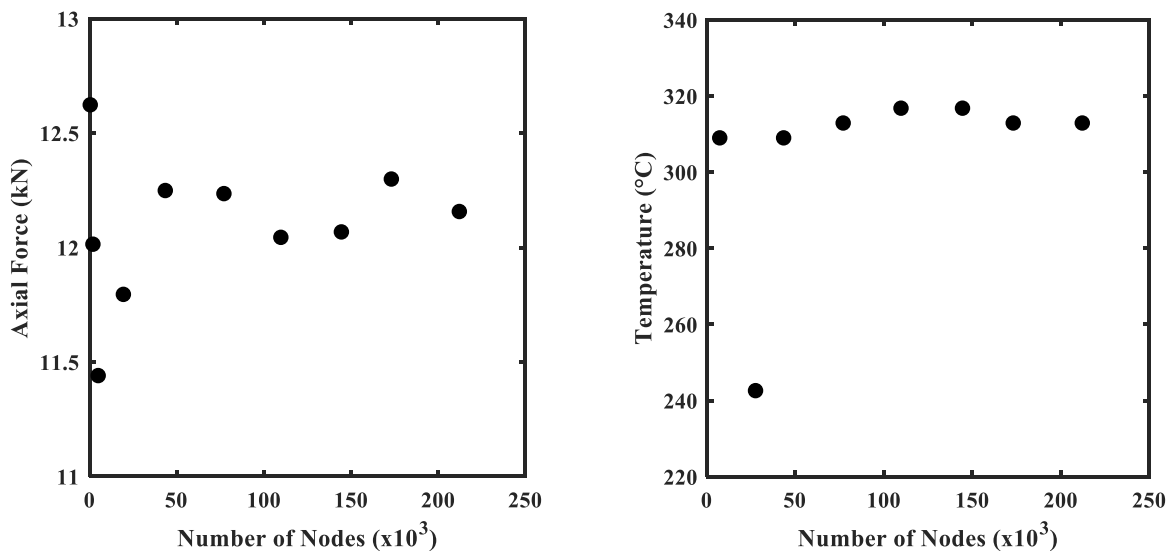


Figure 3: Predicted axial force (left) and critical temperature (right) as a function of the number of nodes

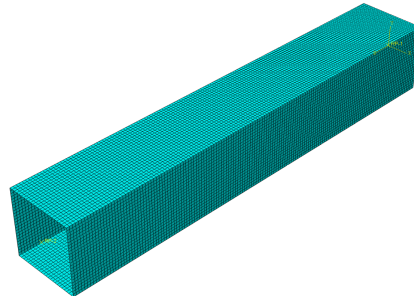


Figure 4: Finite element model with 43,392 nodes and 14400 S8R elements

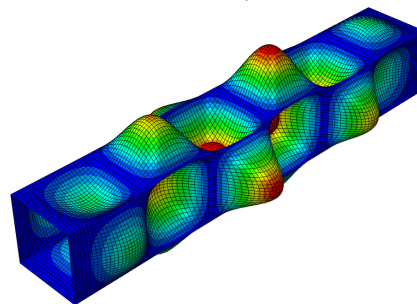


Figure 5: First elastic buckling mode used to define the geometric imperfections

### *2.3 Boundary and Loading Conditions*

The boundary conditions aimed to replicate the testing conditions depicted in the study by Maljaars et al. (2009b), using a fixed bottom and pinned top setup. Reference points were created at the center of the bottom and top faces of the compression member. A rigid body constraint was used to tie the set of nodes on the bottom face and set of nodes on the top face to the bottom and top reference points, respectively. The boundary conditions were then applied only to the reference points. The bottom of the model was completely fixed from displacement and rotation in all directions, while the top was only restricted from displacement except in the axial direction.

#### *2.3.1 Steady-State Models*

All steady-state analysis models used the “Static Riks” method in Abaqus with nonlinear geometry turned on, and the maximum arc length set to 0.1. Geometric imperfections were added using the keyword editor in Abaqus. A uniform temperature field was created in the initial step with eight test temperatures varying from 20 to 310 degrees Celsius. The compressive axial load was incrementally applied to the top reference point until failure.

#### *2.3.2 Transient Models*

The transient-state models used two “Static General” steps and an initial uniform temperature field of 20 degrees Celsius. The first (“load”) step had a time period of 1 and a fixed increment size of 1, corresponding to 0.25 minutes. A compressive axial load was applied at the top reference point during this step. The load magnitude was varied for each specimen based on the ultimate axial forces obtained from the steady-state tests. The second (“temperature”) step had a fixed increment size of 1. The temperature field added to this step had a magnitude according to the heating rate of 7 °C/min, using 200 increments, with each increment corresponding to 0.25 minutes. The same conditions were used in conjunction with both tests conducted with transient-state properties and steady-state properties.

## **3. Model Validation**

The validation model was analyzed under steady-state conditions with mechanical properties from steady-state tests; steady-state conditions with properties from the Aluminum Design Manual; transient-state conditions with mechanical properties from steady-state tests; and transient-state conditions with mechanical properties from transient tests.

The axial force on the top reference point (obtained from the reaction force on the bottom reference point in Abaqus) was plotted as a function of axial displacement for each temperature, under steady-state conditions (Fig. 6). In these plots, the peaks were identified as the axial load-carrying capacity of the member at a given temperature.

Axial displacement as a function of temperature under transient-state conditions using mechanical properties from transient tests were plotted. Each curve in Fig. 7 shows the axial deformation of the member as a function of temperature, while maintaining a constant axial load. The initial axial displacement at 20 °C is negative in all cases due to the contraction produced by the axial (compressive) load. Then, the axial displacements become less negative (or positive) as the temperature increase causes free expansion. The transient analyses were stopped when the

temperature was high enough to weaken the members, and make them unable to carry the load. That temperature was labeled as the critical temperature corresponding to a given axial load.

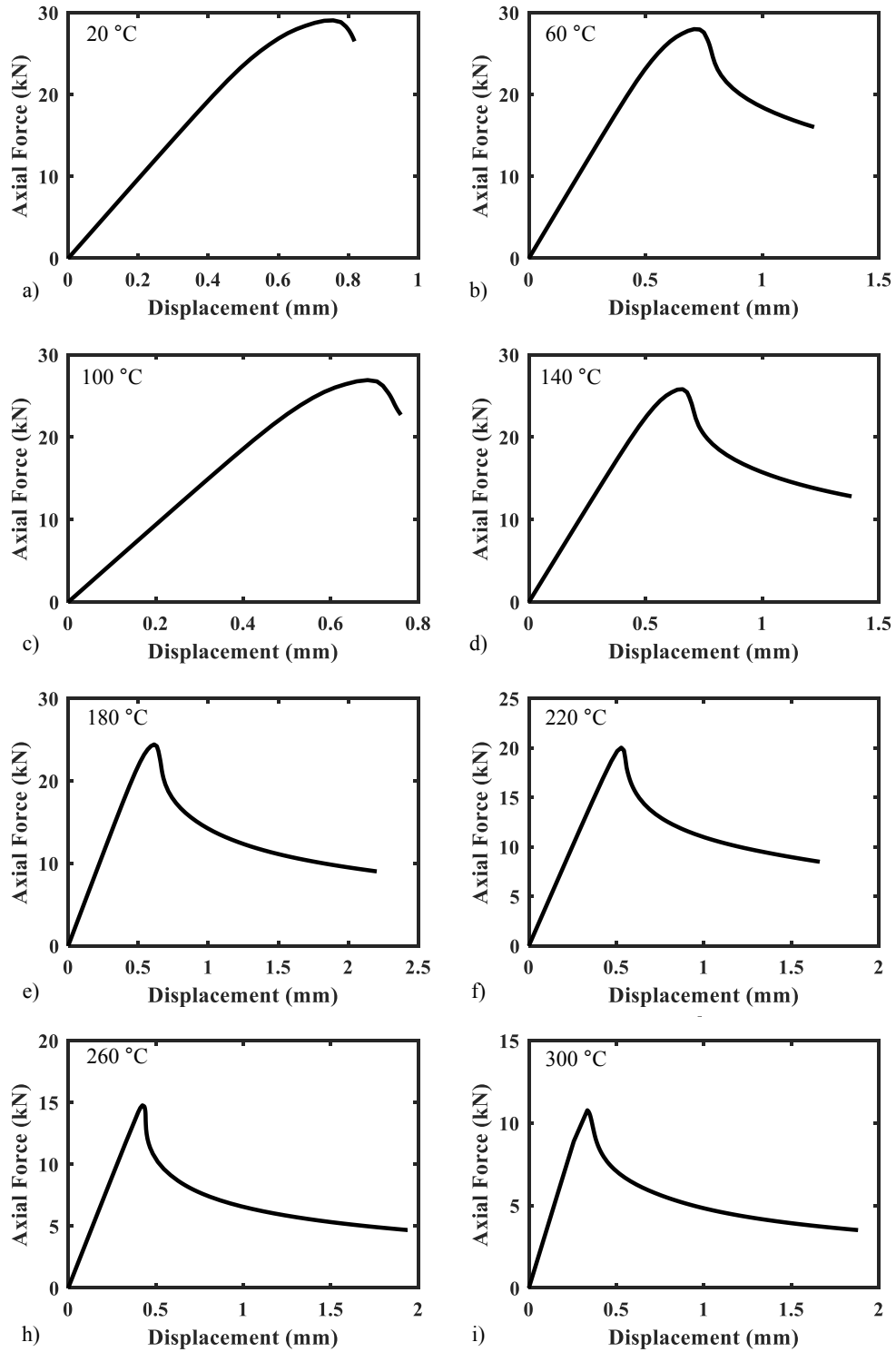


Figure 6: Axial forces and displacement at a given temperature

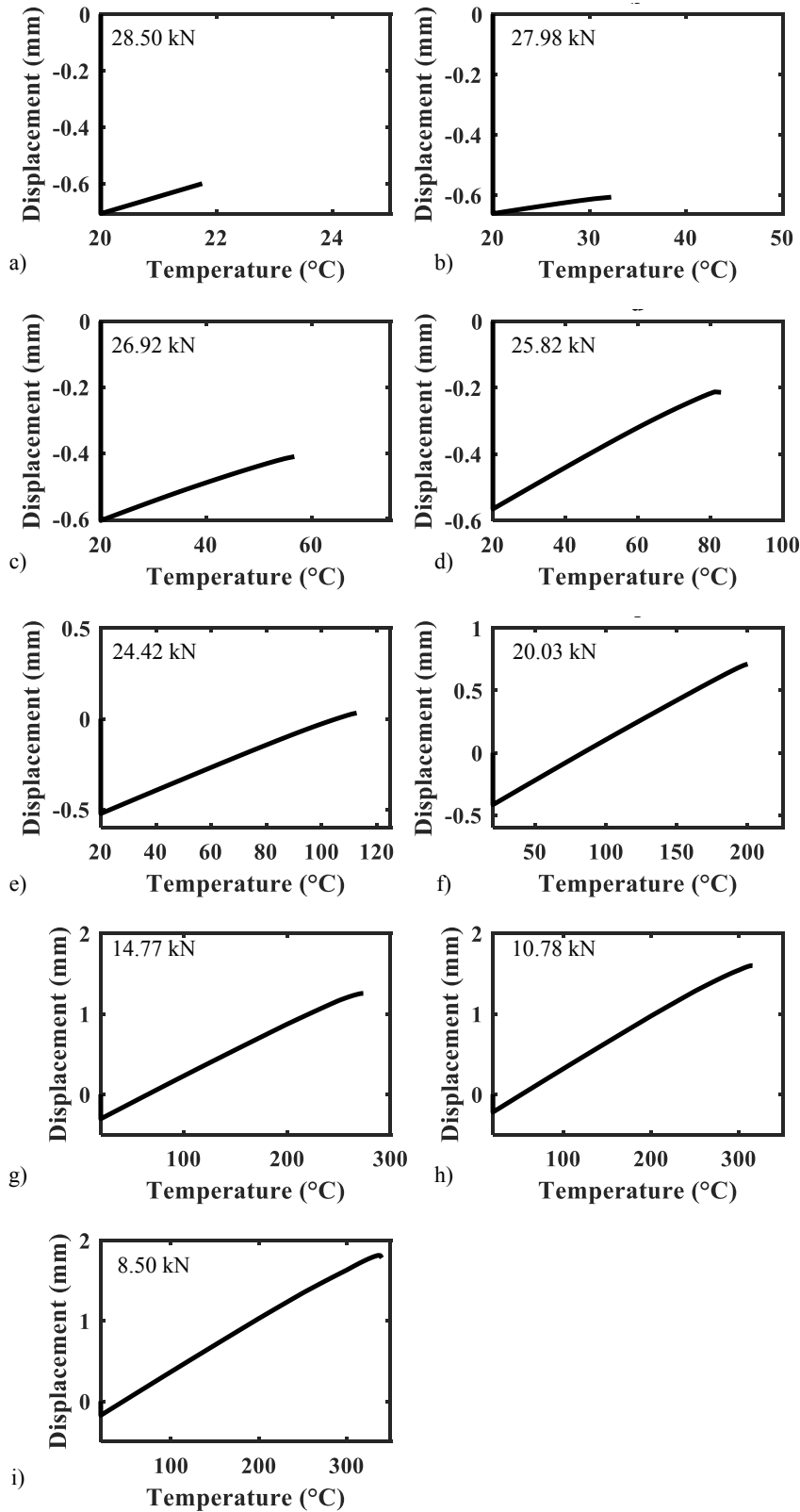


Figure 7: Axial displacement as a function of temperature for a given axial load

Fig. 8 summarizes results from Fig. 6-7 by plotting the axial load-carrying capacity and the corresponding critical temperatures. The load-carrying capacity decreases as the critical temperature increases. In other words, the higher the applied load, the lower the critical temperature is. The same trends are observed regardless of the method (i.e. steady-state or transient) and the mechanical properties assumed (i.e. from steady-state or transient tests). However, in some cases, the predicted load-carrying capacity is inferior when the transient method with mechanical properties from transient tests is adopted.

Predicted load-carrying capacity and critical temperatures predicted through the steady-state or transient method are very similar if mechanical properties from steady-state tests are assumed. Similar results are also obtained by adopting mechanical properties from the Aluminum Design Manual, under steady-state conditions, up to 220 °C. Beyond 220 °C, results based on mechanical properties from the Aluminum Design Manual lead to much lower predicted load-carrying capacity. At 220 °C, experimental results by Maljaars et al. (2009a) coincide with predicted values from numerical models.

#### 4. Parametric Study

Hollow rectangular cross-sections were selected from the Aluminum Design Manual, with dimensions provided in Table 1. Relatively thin sections were chosen so uniform heating could be assumed.

The length of the axial members were 300 mm, 600 mm, and 1200 mm. For the longer members (i.e. 1200 mm long), the first elastic buckling mode was global, and in this case the imperfections were estimated based on the length “ $L$ ”, as  $L/960$ , as recommended by the Aluminum Design Manual (2015).

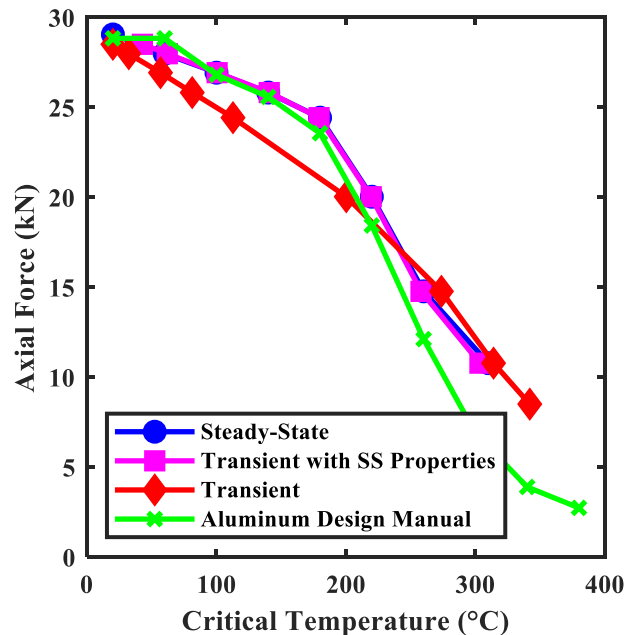


Figure 8: Axial load-carrying capacity and critical temperatures obtained through steady-state or transient analysis, with mechanical properties from steady-state tests, transient tests, or the Aluminum Design Manual

A Poisson ratio of 0.33 is assumed, since it was found that varying this value from 0.3 to 0.4 resulted in less than a 0.5 % difference in the predicted load-carrying capacity, and just over 1.0 % for the critical temperature. The heating rate used was 7 °C/min, with increments every 0.25 minutes. This was determined by taking an average of the “high” heating rates found in the reference study, and rounding to the nearest whole number.

The models provided in Table 1 were tested under steady-state conditions with properties from steady-state tests; transient conditions with properties from steady-state tests; and transient conditions with properties from transient tests. The axial load-carrying capacity was plotted as a function of critical temperature for each of the conditions. The critical temperature was considered the temperature at the maximum displacement, as well as where the velocity changes sign, from positive expansion to negative contraction. The temperature values were measured up to 310 °C, without extrapolating beyond the material properties data available. Sample results are provided below, in Figs. 9 to 12.

The same trends are observed – the load-carrying capacity decreases as the critical temperature is higher. Again, steady-state and “transient” results with mechanical properties from steady-state tests are very similar. In general, results from transient analysis with mechanical properties from transient tests are conservative with respect to steady-state results.

Table 1: Test matrix for square and rectangular sections, including imperfections

Model Name	Height (mm)	Width (mm)	Thickness (mm)	Ratio b/t	Imperfection (mm)	Imperfection Type	Length (mm)
S1	38.1	38.1	1.651	23.08	0.0707	Local	300
S2	38.1	38.1	1.651	23.08	0.0707	Local	600
S3	38.1	38.1	1.651	23.08	1.2500	Global	1200
S4	76.2	76.2	2.413	31.58	0.1034	Local	300
R1	76.2	25.4	3.175	24.00, 8.00	0.1360	Local	300
R2	76.2	25.4	3.175	24.00, 8.00	0.1360	Local	600
R3	76.2	25.4	3.175	24.00, 8.00	1.2500	Global	1200
R4	76.2	50.8	3.175	24.00, 16.00	0.1360	Local	300

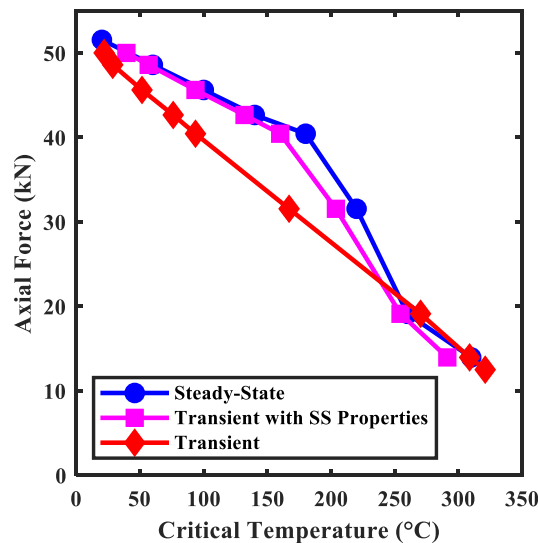


Figure 9: Axial force as a function of the critical temperature for steady-state and transient models S1

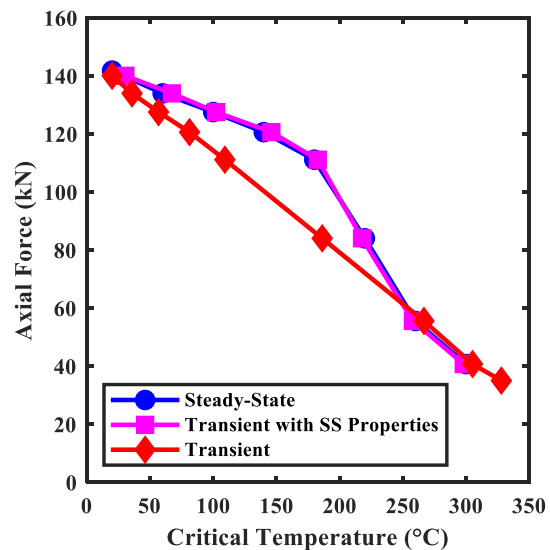


Figure 10: Axial force as a function of the critical temperature for steady-state and transient models S4

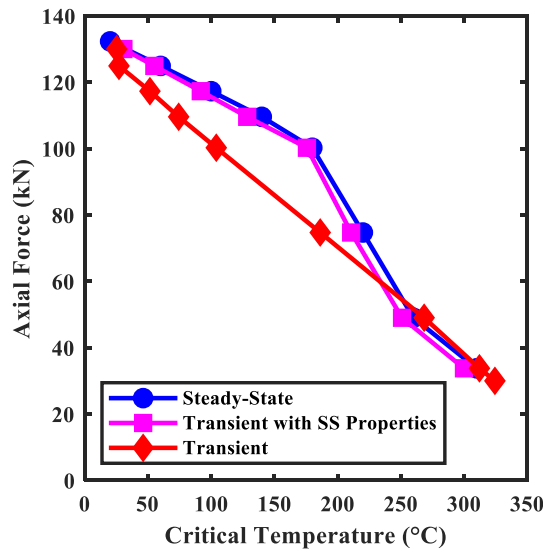


Figure 11: Axial force as a function of the critical temperature for steady-state and transient models R1

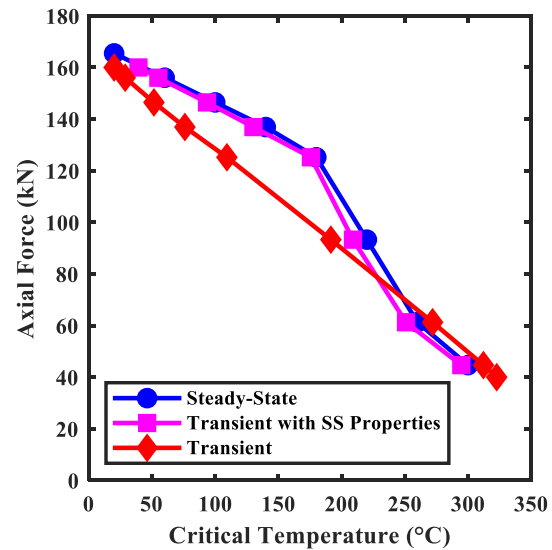


Figure 12: Axial force as a function of the critical temperature for steady-state and transient models R4

## 5. Discussion and Conclusions

In the validation model, the transient tests with mechanical properties from transient tests produced conservative results compared to the steady-state tests until about 260 °C. The steady-state and transient tests with steady-state properties were nearly identical for all temperatures – which means that, the degradation of mechanical properties controls for these relatively short members. Also, steady-state tests with mechanical properties obtained from the Aluminum Design Manual were the most conservative above 220 °C.

If transient models better replicate the real-life response of aluminum members at elevated temperatures, the results obtained in this study show that steady-state models overpredict the load-carrying capacity of members up to 220 °C. The same conclusion applies when mechanical properties from the Aluminum Design Manual are adopted. However, at relatively higher temperature, results from models adopting mechanical properties from the Aluminum Design Manual significantly underpredict the load-carrying capacity of aluminum members when compared against results from transient or steady-state test with experimental 6060-T66 mechanical properties.

Results from “transient” and steady-state models based on mechanical properties from steady-state tests yield very similar results. This observation suggests that numerical models developed with the purpose of simulating transient conditions during a fire, should incorporate mechanical properties obtained from transient tests.

Future work aims to extend the parametric study to include other common aluminum sections and alloys with different temperature-dependent degradation of mechanical properties. Subsequent investigations will seek to utilize numerical models to assess the effects of fire on aluminum structures.

## References

- “Abaqus/CAE” v. 2018, Dassault Systems.
- Aluminum Design Manual: 2015, Aluminum Association.
- Maljaars, J., Soetens, F., Snijder, H.H. (2009a). “Local buckling of aluminum structures exposed to fire. Part 1: Tests.” *Thin-Walled Structures* 47 (11)1404-1417.
- Maljaars, J., Soetens, F., Snijder, H.H. (2009b). “Local buckling of aluminum structures exposed to fire. Part 2: Finite element models.” *Thin-Walled Structures* 47 (11) 1418-1428.
- Mitchell, M., Muftakhidinov, B., Winchen, T. (2018). "Engauge Digitizer Software." Webpage: <http://markumitchell.github.io/engauge-digitizer>, Last Accessed: August 2, 2018
- Skejić, D., Ćurković, I., Rukavina, M. J. (2015). “Behaviour of Aluminium Structures in Fire: A review.” *Applications of Structural Fire Engineering*, Dubrovnik, Croatia